# Observation of Hot-Electron Shot Noise in a Metallic Resistor

Andrew H. Steinbach and John M. Martinis
*National Institute of Standards and Technology, Boulder, Colorado 80303*

Michel H. Devoret
*Service de Physique de l'Etat Condensé, Commissariat à l'Energie Atomique Saclay, F-91191 Gif-sur-Yvette Cedex, France*
(Received 12 January 1996)

We have measured the current noise of silver thin-film resistors as a function of current and temperature and for resistor lengths of 7000, 100, 30, and 1 $\mu$m. As the resistor becomes shorter than the electron-phonon interaction length, the current noise for large current increases from a nearly current independent value to the interacting hot-electron value $(\sqrt{3}/4)2eI$. However, further reduction in length below the electron-electron interaction length decreases the noise to a value approaching the independent hot-electron value $(1/3)2eI$ first predicted for mesoscopic resistors. [S0031-9007(96)00179-2]

PACS numbers: 73.50.Td, 05.30.Fk, 73.23.Ps

Can metallic resistors display shot noise? Shot noise, first discovered in vacuum tubes [1], is a basic manifestation of the discreetness of charge carriers and occurs in many solid state devices such as metal-insulator-metal tunnel junctions [2], Shottky barrier diodes, and *p-n* junctions [3]. This noise arises from electrons traveling independently and randomly (Poisson transport) from one side of the device to the other. In contrast a resistor, i.e., a metallic wire in which the electrons propagate diffusively, is commonly thought not to produce shot noise [4]. In this Letter, we provide the first experimental demonstration that a metallic resistor that is sufficiently small and cold can display several different regimes of shot-noise-like behavior.

Shot noise in an electrical element is characterized by a frequency independent power spectrum $S_I$ of current fluctuations such that $S_I \propto eI$ for large average current $I$ flowing through the element. For a tunnel junction of resistance $R$, $S_I = (2eV/R)\coth(eV/2k_BT)$ [5], which gives Johnson noise $S_I = 4k_BT/R$ for the limit $eV \ll k_BT$ and shot noise $S_I = 2eI$ for $eV \gg k_BT$. Here $V$ and $T$ are the voltage across and the temperature of the junction, respectively.

For a metallic resistor of length $L$ and resistance $R = V/I$ (see Fig. 1), one must distinguish several different regimes according to the relationship between $L$ and four characteristic length scales which describe the progressive loss of reversibility in the electron motion as the length is increased. These length scales are the elastic mean free path $\ell$, the phase breaking length $L_\varphi$, the length in which inelastic collision among the electrons cause their thermalization $L_{e\text{-}e}$, and the length in which the electron temperature can relax to the phonon temperature $L_{e\text{-ph}}$. Typically a metal has $\ell < L_\varphi < L_{e\text{-}e} < L_{e\text{-ph}}$ [6].

Theoretical descriptions of noise in these regimes assume the resistor is attached to ideal thermal and electrical reservoirs at its two ends 1 and 2. These reservoirs impose an electron temperature $T$ and chemical potentials $\mu_1$ and $\mu_2$ such that $\mu_1 - \mu_2 = eV$. Because experimental control of temperature is mediated through phonons, good electron-phonon coupling in the reservoirs is necessary to insure that $T$ is equal to the phonon temperature. Since the electron-phonon relaxation rate per unit length of a long wire is proportional to its cross section, thermal reservoirs are implemented in our samples by making the cross section of the wire increase abruptly at the contact pads, as shown in the inset of Fig. 1.

For $L_{e\text{-ph}} \ll L$ (macroscopic regime), the resistor is large enough so that heat generated in the resistor is

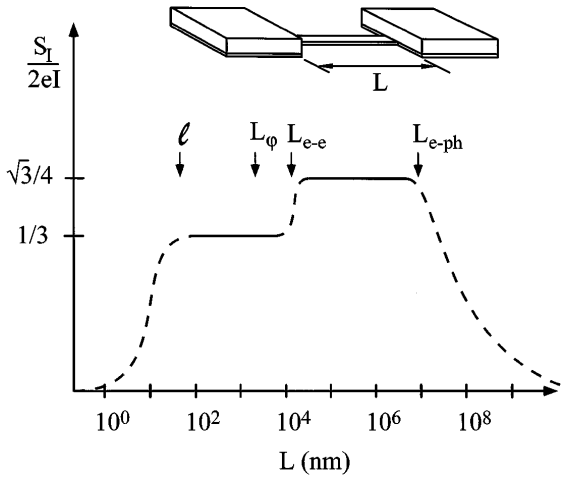


FIG. 1. Theoretical predictions shown in schematic form for $S_I/2eI$ vs sample length $L$ in the regime $eV \gg k_BT$. Solid lines give theoretical predictions as discussed in text. Dashed lines sketch expected behavior in crossover regimes. The arrows pointing to the $L$ axis depict only qualitatively the relative magnitude of the length scales $\ell$, $L_\varphi$, $L_{e\text{-}e}$, and $L_{e\text{-ph}}$; typical values are 50 nm, 1 $\mu$m, 10 $\mu$m, and 10 mm, respectively. The last three values are voltage dependent (see Ref. [6]) and have been estimated for $V = 100$ $\mu$V. Inset illustrates sample geometry and shows the Ag thin-film resistor of length $L$ and contact pads formed by a second, thicker Ag layer.

directly removed by phonons and the electron temperature throughout the resistor is thus $T$. The noise is $S_I = 4k_BT/R$, independent of $I$, and thus the resistor displays no shot noise as commonly expected [4]. For $L_{e\text{-}e} \ll L \ll L_{e\text{-ph}}$ (which we call the interacting hot-electron regime), the electrons become hot due to Joule heating and thermalize their energy via electron-electron interactions. Their cooling occurs only by thermal conduction to the reservoirs [7,8], described by the Wiedemann-Franz law [9], which then gives a temperature profile inside the resistor. A Johnson noise calculation then predicts [7] $S_I = (2k_BT/R)[1 + (v + 1/v)\tan^{-1}v]$, where $v = \sqrt{3}eV/2\pi k_BT$, giving $S_I = (\sqrt{3}/4)2eI$ for $eV \gg k_BT$. For $L_\varphi \ll L \ll L_{e\text{-}e}$ (which we call the independent hot-electron regime), the electrons do not interact and thus behave independently. They are still hot but no longer have a Fermi distribution. There, one predicts [10] $S_I = (2/3)[4k_BT/R + (eV/R)\coth(eV/2k_BT)]$, giving $S_I = (1/3)2eI$ for $eV \gg k_BT$. For $\ell \ll L \ll L_\varphi$ (mesoscopic regime), the resistor cannot be described by a classical population function. But surprisingly, mesoscopic theory predicts the same result as in the independent hot-electron case [11]. Finally for $L \ll \ell$ (the ballistic or point-contact regime), the shot-noise contribution vanishes except for one-channel effects [12,13].

Because noise in the regime $L \ll L_{e\text{-ph}}$ is proportional to $eI$ and arises from electrons which are excited above the temperature $T$, we call this effect hot-electron shot noise.

We summarize the $L$ dependence of hot-electron shot noise in Fig. 1. As $L$ is decreased from the macroscopic limit, the hot-electron shot noise first increases from 0 in the macroscopic regime to a value of $0.87eI$ in the interacting hot-electron regime, and then decreases slightly to $0.67eI$ in the independent hot-electron and mesoscopic regime. Note that shot noise in a metallic wire has a maximum value of $0.87eI$, and these universal results depend critically on the presence of ideal thermal reservoirs at both ends of the resistor.

A previous experiment has measured the noise from self-heating in long metallic wires at low temperatures [14], but did not implement the ideal thermal reservoirs discussed above. In two-dimensional electron gas (2DEG) samples thermal reservoirs are routinely implemented in various transport experiments [15]. A recent experiment measured the noise in a 2DEG sample and showed that it was proportional to current and consistent with the $0.67eI$ prediction [16]. However, this measurement gave a coefficient of $eI$ that varied between 0.4 and 0.8 with gate voltage. Our experiment is the first to measure the shot noise with sufficient accuracy to distinguish between the $0.67eI$ and $0.87eI$ predictions and to demonstrate the length dependence. These results were achieved by using a novel low-noise, high-bandwidth SQUID preamplifier [17] and by carefully accounting for systematic errors to obtain an absolute measurement of the current noise accurate to 2%. In particular, the measurement of the temperature dependence of the noise was essential for the verification of our absolute calibration.

We have measured the current noise in four Ag thin-film resistors of lengths $L = 1$, 30, 100, and 7000 $\mu$m. Each resistor had the same nominal thickness $t = 0.05$ $\mu$m, a width $w$ such that $L/w \approx 10$, and consequently had similar resistances $R \approx 1\ \Omega$. In order to make the two 1 cm$^2$ contact pads as near as possible to ideal thermal reservoirs, they were augmented by a second Ag layer for a total thickness of 0.5 $\mu$m. The initial layer was argon-ion sputter cleaned prior to the second deposition to ensure good electrical contact. Optical lithography was used for all fabrication steps except for the 1 $\mu$m resistor which was fabricated with $e$-beam lithography.

SQUID amplifiers are well suited to measure the current noise of these low impedance samples at dilution refrigerator temperatures. Our SQUID amplifier consisted of a single dc SQUID input stage followed by a 100 SQUID series-array output stage [17]. This SQUID system was operated in a flux-locked loop and had a bandwidth exceeding 100 kHz.

The idealized schematic of the noise measurement system (see upper inset of Fig. 2) consists of the sample in series with the superconducting input coil of the SQUID and a bias voltage $V$. The SQUID measures the dc current $I = V/R$ and the noise current $i_n$ shown as a current source in parallel with the sample.

In the actual measurement system (lower inset of Fig. 2) the noise current $i_n$ does not entirely flow through the SQUID input coil due to the nonzero resistance $R_{\text{stray}}$ of the circuit shunting the sample. This shunt circuit includes the stray wiring resistances $R_{\text{still}}$ and $R_{\text{mix}}$ as well as the finite resistance of the voltage divider $R_2 \| R_1 \approx R_2$,

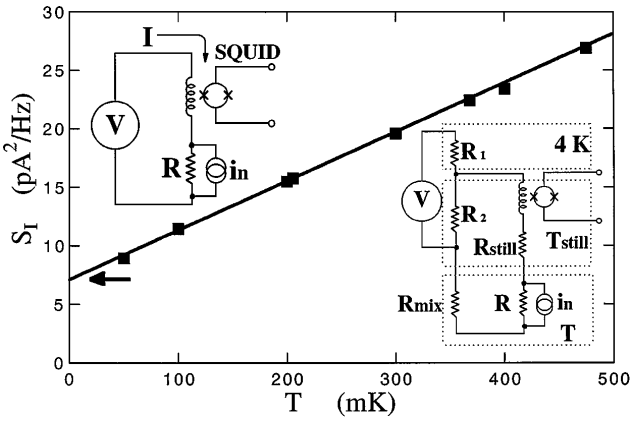


FIG. 2. Plot of the resistor current noise $S_I$ at $I = 0$ vs reservoir temperature $T$ for the $L = 1$ $\mu$m sample. Solid line gives Johnson noise prediction obtained from our measured resistance. The prediction is offset by 7 pA$^2$/Hz (arrow), the noise of the entire measurement system. Upper (lower) inset shows schematic of the idealized (actual) measurement system. Typical resistance values are $R_1 = 2$ k$\Omega$, $R_2 = 0.07\ \Omega$, $R_{\text{still}} = 0.007\ \Omega$, $R_{\text{mix}} = 0.01\ \Omega$, and $R = 1\ \Omega$.

giving $R_{\text{stray}} = R_{\text{still}} + R_{\text{mix}} + R_2$. These resistances as well as the sample were measured with voltage taps (not shown) for each chip. The current noise measured by the SQUID is $S_I^{\text{meas}} = [R/(R + R_{\text{stray}})]^2 S_I(I,T) + [R_{\text{mix}}/(R + R_{\text{stray}})]^2 4k_B T/R_{\text{mix}} + \text{const}$ terms, where $S_I(I,T)$ is the spectral density of the current noise $i_n$ of the sample.

The SQUID input current to output voltage conversion was calibrated in a separate experiment. Measurements with a spectrum analyzer showed that the noise was white from approximately 1 to 100 kHz. The spectral density $S_I^{\text{meas}}$ was then obtained by averaging between 10 and 50 kHz. The uncertainty in $S_I$ is approximately equal to the size of the plotted data points.

We verified that every sample exhibited the predicted Johnson noise behavior at zero current bias in order to check the absolute calibration of the entire measurement system. Figure 2 shows the $T$ dependence of $S_I$ at $I = 0$ for the $L = 1$ $\mu$m sample. The $S_I$ value extrapolated to $T = 0$ (arrow) gives the measurement system noise. The solid line predicts the noise arising from the measurement system and the Johnson noise $4k_B T/(R + R_{\text{mix}})$ calculated from the measured resistances. The slope of the data and prediction agree to within 2%. This level of agreement was obtained for all the samples.

The spectral density as a function of current for the $L = 30$ $\mu$m sample is shown in Fig. 3 for three temperatures. Because the measurement system noise may drift by 5% between current sweeps at different temperatures, we have plotted the data as the variation of noise with current. However, we also offset each data sweep by $4k_B T/R$ to display the variation with temperature of the high current data. The theoretical predictions of the interacting hot-electron regime, which have no adjustable parameters, are given by the solid lines and agree well with the data. In particular, the two lowest temperature data sets approach one another at high current, while the highest temperature data set remains separated, as predicted by theory. The prediction for the independent hot-electron regime (dotted line) at the lowest temperature is shown for comparison and is incompatible with the data.

In order to verify the predictions of the independent hot-electron regime, one must fabricate a sample with $L \ll L_{e\text{-}e}$. In Fig. 4 we show data for $L = 1$ $\mu$m, the shortest length for which we can readily fabricate a sample. Along with the data we show the theoretical predictions for the independent (dotted) and interacting (solid) hot-electron regimes. At the two highest temperatures both data and theory have been offset by a constant amount for clarity. The 50 mK data clearly fall below the interacting hot-electron prediction and establish the existence of a regime where the noise is suppressed, presumably because of fewer electron-electron interactions. We believe that the data lie above the independent electron prediction because residual electron-electron interactions are still present. We estimate that the spreading resistance or heating of the contact pads can account only for a slope change of $+0.04eI$ and thus cannot account fully for the deviation.

Another decrease in noise from the interacting hot-electron prediction is also expected for long samples in which the electron-phonon interaction appears. Figure 5 shows our data for the $L = 7$ mm and 100 $\mu$m samples. The 7 mm sample is well into the macroscopic limit $L_{e-\text{ph}} \ll L$, and shows a current noise well below the hot-electron shot noise predictions. The current noise is not independent of $I$ because the electron-phonon interaction is not strong enough to completely thermalize the electrons to the phonon temperature. The position dependent electron temperature was computed by solving numerically the one-dimensional heat diffusion equation

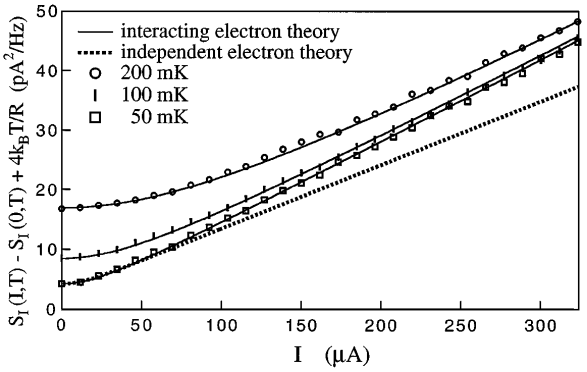


FIG. 3. Variation of $S_I(I,T)$ vs $I$ for the $L = 30$ $\mu$m sample at $T = 50$, 100, and 200 mK . Sample resistance $R = 0.68$ $\Omega$. Data show good agreement with the interacting hot-electron theory (solid curves) with no adjustable parameters. The independent hot-electron theory for 50 mK (dotted curve) is also plotted and shows poor agreement.

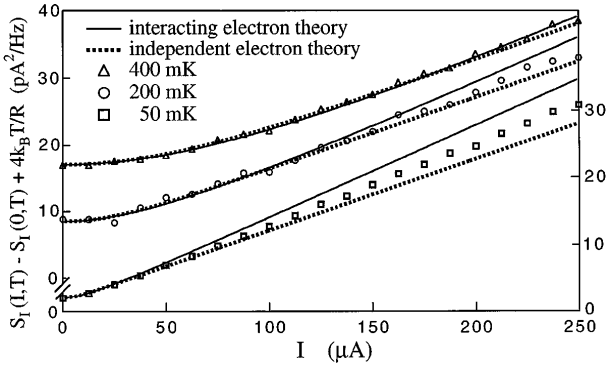


FIG. 4. Variation of $S_I(I,T)$ vs $I$ for the $L = 1$ $\mu$m sample at $T = 50$, 200, and 400 mK. Sample resistance $R = 1.31$ $\Omega$. Predictions for interacting (solid curves) and independent (dotted curves) hot-electron theory are shown for comparison. Data and theory at 200 and 400 mK are offset for clarity. Suppression of the noise below the interacting hot-electron theory shows that the electron energies are not thermalizing via electron-electron interactions.

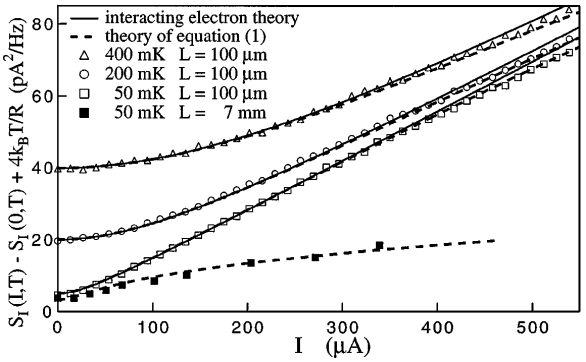


FIG. 5. Variation of $S_I(I,T)$ vs $I$ for the $L = 100$ $\mu$m sample at $T = 50$, 200, and 400 mK, and for the $L = 7$ mm sample at $T = 50$ mK. Sample resistances are $R = 0.57$ and 0.90 $\Omega$, respectively. Solid curves give interacting hot-electron predictions for the $L = 100$ $\mu$m sample. Dashed curves give predictions of Eq. (1) with $\Sigma = 0.5$ nW/$\mu$m$^3$ K$^5$ and show good agreement with data.

for constant cross section

$$L^2 \frac{d}{dx}\left(\frac{\mathcal{L}\,T_e}{R}\,\frac{d}{dx}\,T_e\right) = -\frac{V^2}{R} + wtL\Sigma(T_e^5 - T^5), \quad (1)$$

where $x$ is the position along the wire, $T_e(x)$ is the electron temperature, $\mathcal{L} = \pi^2 k_B^2/3e^2$ is the Lorenz number [9], and $\Sigma$ characterizes the electron-phonon coupling [14]. The boundary conditions are $T_e(0) = T_e(L) = T$ since the pads have been made as close as possible to heat reservoirs. The current noise can then be obtained from $S_I = 4k_B\langle T_e(x)\rangle/R$, where $\langle T_e(x)\rangle = \int_0^x T_e(x)dx/L$ is the average temperature. The characteristic scale $L_{e\text{-ph}} = (16k_B/\sqrt{3}e)^{5/2}(\sigma/V^3\Sigma)^{1/2}$ is estimated by equating the two terms of the right-hand side of Eq. (1) and by setting $4k_BT_e/R = \sqrt{3}eI/2$ and $T = 0$. Here, $\sigma = L/wtR$ is the conductivity of the thin-film resistor. Equation (1) can be readily generalized for nonuniform cross section. However, in the limiting case $\Sigma = 0$ the noise becomes independent of variations of cross section and therefore adopts the universal (i.e., shape independent) interacting hot-electron result.

This theory was used to fit the $L = 7$ mm data in Fig. 5 using $\Sigma$ as an adjustable parameter. The best fit value $\Sigma = 0.5$ nW/$\mu$m$^3$ K$^5$, compatible with other measurements [14], gave a prediction that describes well the experimental data. This value of $\Sigma$ was then used in turn to predict the noise for the $L = 100$ $\mu$m sample, also shown in Fig. 5 by a dashed line. The dashed lines clearly describe the data much better than the solid lines which correspond to the $\Sigma = 0$ prediction.

In conclusion, we have made the first hot-electron shot noise measurement on metallic wires with sufficient accuracy to distinguish between the values predicted in different wire-length regimes. Shot noise appears when the length of the wire is decreased to a value comparable with the electron-phonon interaction length. As the sample length is decreased further the spectral density of the noise reaches the maximum $(0.87 \pm 0.02)eI$ which matches the predition for electrons decoupled from the phonons but still interacting among themselves. As the sample length is finally reduced to mesoscopic dimensions, our data clearly demonstrate a reduction of the shot noise. The reduction is compatible with a crossover between the $0.87eI$ and $0.67eI$ values of the interacting and independent hot-electron regimes. Finally, this experimental technique could provide a direct and independent measurement of the electron-electron interaction in thin metal films.

We would like to acknowledge useful discussions with M. de Jong, D. Esteve, C. Glattli, R. Liu, and D. Prober. This work was supported in part by the Office of Naval Research under Contract No. N000014-94-0087.

[1] W. Schottky, Ann. Phys. (Leipzig) **57**, 541 (1918).
[2] H. Birk, M. J. M. de Jong, and C. Schonenberger, Phys. Rev. Lett. **75**, 1610 (1995).
[3] A. van der Ziel, *Noise in Solid State Devices and Circuits* (Wiley, New York, 1986).
[4] P. Horowitz and W. Hill, *The Art of Electronics* (Cambridge University Press, Cambridge, 1989), p. 432.
[5] D. Rogovin and D. J. Scalapino, Ann. Phys. (N.Y.) **86**, 1 (1974).
[6] B. L. Al'tshuler, A. G. Aronov, and D. E. Khmelnitsky, J. Phys. C **15**, 7367 (1982); B. L. Al'tshuler, A. G. Aronov, D. E. Khmelnitsky, and A. I. Larkin, in *Quantum Theory of Solids*, edited by I. M. Lifshitz (Mir, Moscow, 1982). These authors discuss $\tau_\varphi$, $\tau_{e\text{-}e}$, and $\tau_{e\text{-ph}}$, but the relationship with $L_\varphi$, $L_{e\text{-}e}$, and $L_{e\text{-ph}}$ is easily obtained through $L_x = \sqrt{D\tau_x}$ where $D$ is the diffusion constant.
[7] A. Steinbach, J. Martinis, and M. Devoret, Bull. Am. Phys. Soc. **40**, 400 (1995); M. J. M. de Jong, Ph.D. thesis, Leiden University, 1995; K. E. Nagaev, Phys. Rev. B **52**, 4740 (1995); V. I. Kozub and A. M. Rudin, Phys. Rev. B **52**, 7853 (1995).
[8] D. E. Prober, M. N. Wybourne, and M. Kansakar, Phys. Rev. Lett. **75**, 3964 (1995).
[9] C. Kittel, *Introduction to Solid State Physics* (Wiley, New York, 1986).
[10] K. E. Nagaev, Phys. Lett. A **169**, 103 (1992).
[11] C. W. J. Beenakker and M. Buttiker, Phys. Rev. B **46**, 1889 (1992).
[12] M. Buttiker, Phys. Rev. Lett. **65**, 2901 (1990).
[13] Y. P. Li *et al.*, Appl. Phys. Lett. **57**, 774 (1990); S. Washburn *et al.*, Phys. Rev. B **44**, 3875 (1991); M. Reznikov *et al.*, Phys. Rev. Lett. **75**, 3340 (1995); A. Kumar *et al.*, Phys. Rev. Lett. **76**, 2778 (1996).
[14] M. L. Roukes, M. R. Freeman, R. S. Germain, R. C. Richardson, and M. B. Ketchen, Phys. Rev. Lett. **55**, 422 (1985).
[15] C. W. J. Beenakker and H. van Houten, in *Solid State Physics* (Academic Press, Boston, 1991), Vol. 44.
[16] F. Liefrink, J. I. Dijkhuis, M. J. M. de Jong, L. W. Molenkamp, and H. van Houten, Phys. Rev. B **49**, 14 066 (1994).
[17] R. P. Welty and J. M. Martinis, IEEE Trans. Appl. Supercond. **3**, 2605 (1993).